# BEAM HALO STUDIES FOR CTF3

C.P. Welsch#, University of Liverpool and the Cockcroft Institute, UK
S. Artikova, Max Planck Institute for Nuclear Physics, Heidelberg, Germany
R. Fiorito, A. Shkvarunets, H. Zhang, UMD, College Park, Maryland, USA

*Abstract*

Beam halo can have severe effects on the performance of high energy accelerators. It reduces the experimental throughput, may lead to noise in the experiments, or even damage accelerator components. In order to understand and ideally control the formation and evolution of beam halo, detailed studies are required.

In this contribution halo generation mechanisms and the underlying physical principles are first presented, before the particular case of the CLIC Test Facility (CTF3) is discussed. The results from test measurements at UMER, based on an adaptive mask that is used to filter out the beam core, are presented.

## INTRODUCTION

Uncontrolled beam loss leads to excessive radioactivation in high intensity and high energy accelerators. For a well controlled beam, losses are typically associated with a low density halo surrounding the beam core. There are many mechanisms which contribute to halo formation. Various machine non-linearities and misalignments, rms mismatch, space-charge coupling resonances, space-charge induced structure resonances, Coulomb scattering within the beam and on the residual gas, and collective instabilities are some of the relevant sources of halo generation. In addition to these sources, beam injection, foil stripping and extraction, as well as RF noise, mechanical imperfections and lattice resonances often cause halo built-up in accelerators [1].

It is important to understand the different sources of beam halo formation, investigate into which of them might have significant impact on the operation of a specific machine, and to find ways of suppressing or controlling these effects.

The structure of beam halo and its characteristics depend strongly on its formation mechanism. It is important to understand these mechanisms and to have the possibility to benchmark any model through experimental studies. For this purpose, the beam profile needs to be monitored with a dynamic range of at least $10^4$ to allow for a sufficient level of detail in the tail regions of the beam distribution.

## THE TBL AT CTF3

CTF3 has been constructed at CERN by an international collaboration [2]. It shall demonstrate the key technological challenges for the construction of a high luminosity 3 TeV $e^+$-$e^-$ collider. The first part of this test facility generates a high current beam of almost 30 A. This beam has a pulse length of 140 ns and is bunched at 12GHz. It is then transported to the CLic Experimental area (CLEX). One of the critical issues under investigation is the reliability and efficiency of the RF power production. Within CLEX, this is addressed in the so-called Test Beam Line (TBL) [3], Fig. 1.

Figure 1: Photograph of the test beam line at CTF3.

Built in stages, with a first Power Extraction and Transfer Structure (PETS) module installed in 2009, the TBL will experimentally characterize the stability of the drive beam during deceleration. Its rather simple lattice allows for numerical tracking of complex beam distributions. The beam line has several diagnostics ports, including OTR screens, and thus allows for measuring the beam profile at different locations. This is an ideal frame for benchmarking numerical studies against experimental data.

## HALO MONITORING

Optical Transition Radiation (OTR) is particularly suited for the observation of the beam intensity distribution, because of its fast time response and very good linearity with the beam signal over a wide intensity range. It is produced when charged particles pass through media with different dielectric constants.

A beam profile measured by detecting OTR light after suppressing the beam core with a fixed mask is shown in Fig. 2.

Although limited in flexibility since the mask cannot be adapted to the respective beam shape, this setup allow for the demonstration of an increase in dynamic range by a factor of ten as compared to the conventional beam profile monitor at the same location [4].

#carsten.welsch@quasar-group.org

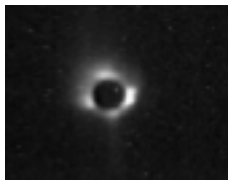

Figure 2: Image of beam Halo measured at CTF3 with fixed mask [4].

Based on these initial studies, tests with advanced camera systems, such as Thermo Fisher's SpectraCAM XDR, were carried out [5] and in parallel, measurements with an adapative mask based on a micro mirror array were started [6].

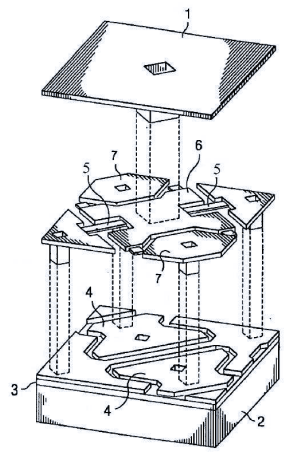


Figure 3: Image of beam Halo measured at CTF3 with fixed mask [7].

The Micro Mirror Array used for these measurements consists of an array of 1024×768 micro mirrors of 13.68µm×13.68µm size. Each of them can individually be set to ±12°. Light will then be reflected in different directions depending on the micro mirror state. It is thereby possible to use the MMA as an adjustable mask.

Each single pixel of the MMA can be separated in a substructure and superstructure. The mirror itself is attached to the superstructure. The substructure of the pixels consists of a silicon substrate (Fig.3-2) with an insulating layer (Fig.3-3) on top, which isolates the superstructure from the substructure. Upon the insulating layer, there is a thin metallic layer, which forms the lower address electrodes (Fig.3-4) and also supports the hinge. The hinge consists of the flexible torsion beam (Fig.3-5), the large hinge yokes (Fig.3-6), and upper address electrodes (Fig.3-7). If there is an appropriate potential applied to the upper and the lower electrodes (Fig.3-4; 3-7), the electrostatic force between them induces a torque and causes the hinge to tilt. The torsion beam (Fig.3-5) acts as a torsion spring and creates a resisting torque. The hinge is tilted until the resisting torque of the torsion spring and the electrostatic torque are of the same magnitude or until it is stopped mechanically by touching the substructure. Since the pixel is used only in a digital ON-OFF mode, the voltage between the two electrodes is set high enough to cause the maximum deflection.

The mask generation process is illustrated in Fig. 4. The profile of the beam is first measured with all mirrors activated, so that all light is detected by the camera. Since the MMA only has two different states it can be set to, the grayscale image needs then to be converted into a binary image to define the mask. The threshold value that decides on whether a pixel belongs to the core or the tail distribution can be set freely. This binary image is then sent to the MMA and defines the position of the mirrors. In a final step, the image is the re-measured with the mask and an increased dynamic range.

It should be noted that, in addition to the above procedure, the different size and orientation of the MMA and the camera chip need to be taken into account. Therefore, a coordinate transformation is required during the process.

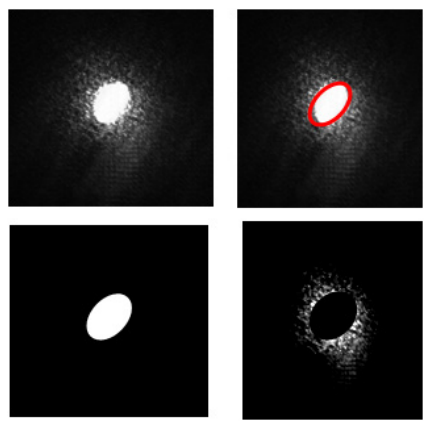

Figure 4: Illustration of the mask generation process: Beam profile is measured (top left), mask defined according to threshold value (top right), mask is displayed on MMA (bottom left), profile is re-measured with increased dynamic range (bottom right).

## EXPERIMENTAL RESULTS AT UMER

Earlier lab measurements with a laser that simulate the OTR light in CTF3 indicated that the MMA might introduce a diffraction pattern both in the core of the beam distribution and the tail region [6]. If this was the case, the detector itself would change the beam characteristics.

Investigation into such problems at CTF3 is not easy: The radiation level in the machine is rather high and thus installations and modifications are not easy to realize.

Therefore, measurements with beam were carried out at the University of Maryland Electron Ring (UMER). This low energy (10 keV) accelerator guarantees stable beam storage over long storage times, is well studied and allows for simple access to the accelerator and rather easy integration of new diagnostics equipment.

At UMER, light from a scintillating screen was used to monitor the transverse beam profile. A flexible optics consisting of several lenses was installed to allow for adjusting the focus and magnification on the MMA and the camera chip independently. As a first step, the MMA was used to deflect the beam entirely, Fig. 5 (right). It can be seen that no pattern was found and therefore earlier concerns that arose in lab measurements using a laser were not confirmed with the incoherent light from the phosphor screen used at UMER.

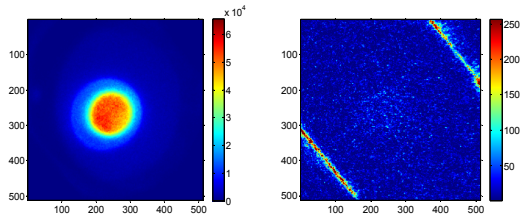

Figure 5: Measured beam profile without (left) and with mask (right).

The system was then used to monitor the beam profile with different mask sizes. The background obtained when the beam was turned off was subtracted and averaging over 10 pixels was applied to smooth the signal. The signal in the tail of the distribution was increased by extending the measurement time of the ICCD camera progressively for each mask size. The result of these measurements is indicated in Fig 6 and a reconstruction of the beam profile shown in Fig. 7.

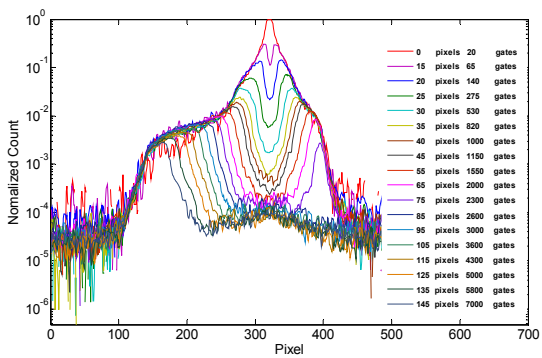


Figure 6: Measured beam profile with different mask sizes. Background subtraction and signal averaging was applied.

It should be noted that the measurement at CTF3 would be done in a different way. The light level at CTF3 is far higher than at UMER. This will allow the use of a conventional (and cheap) CCD camera. The initial beam profile will then be measured with optical density filter introduced into the light path in a way that the CCD is as close as possible to saturation to avoid charge overflow and blooming effects. After the definition of the mask, the OD filters will be removed to allow the camera to reach close to saturation again – this time with the same image acquisition time. By using increasing mask sizes and changing the OD filter setting, the full beam profile can then be reconstructed with high dynamic range.

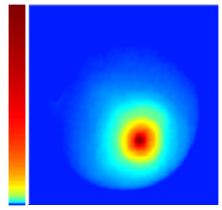

Figure 7: Reconstructed beam profile; logarithmic intensity scale. The dynamic range is close to $10^5$ with a very small noise level.

## CONCLUSION AND OUTLOOK

The understanding and possible control of beam halo is important for essentially all accelerators. It is crucial for the operation of high energy, high intensity accelerators where beam loss can cause critical damage to the machine. A beam halo monitor based on a micro-mirror array was developed and used for first tests with beam at the UMER facility in Maryland. These measurements indicate a dynamic range of more than $10^4$ and thus confirm previous lab results.

The TBL at CTF3 allows for the controlled deceleration of an intense beam in a rather simple lattice. It contains a number of diagnostics ports, allowing for the integration of a high dynamics range beam profile monitor at different positions. Such measurements will allow benchmarking numerical models of halo propagation with experimental results and to further the understanding of the beam dynamics in accelerators.

## ACKNOWLEDGEMENTS

The authors would like to thank their DITANET partners CERN, Thermo Fisher Scientific and ViALUX for the fruitful collaboration and continuous support.

## REFERENCES

[1] C.P. Welsch et al., "Alternative techniques for beam halo measurements", Meas. Sci. Technol. **17** (2006) 2035–2040.

[2] G. Geschonke et al. CTF3 Design Report,CERN/PS 2002-08 (2002).

[3] S. Döbert, G. Rumolo, D. Schulte, I. Syratchev, D. Carrillo, "Progress on the CTF3 Test Beam", Proc. EPAC, Edinburgh, Scotland (2006).

[4] T. Lefèvre, et al., "Beam halo monitoring at CTF3", Proc. Europ. Part. Acc. Conf., Lucerne, Switzerland (2004).

[5] C.P. Welsch, et al., "A beam halo monitor based on adaptive optics", Proc. SPIE 6616 (2007) 9.

[6] J. Egberts et al., "Flexible core masking technique for beam halo measurements with high dynamic range", JINST **5** P04010 (2010).

[7] T.J. Meyer, B.A. Mangrun and M.F. Reed, "Split Beam Micromirror", Texas Instruments Inc. (2006).

[8] R. Fiorito et al, "Beam Halo Imaging with an Adaptive Optical Mask", Proc. BIW, Santa Fe, USA (2010).